SCIENTIFIC REPORTS

OPEN

SUBJECT AREAS:
PROSTATE CANCER
MECHANISMS OF DISEASE
TRANSLATIONAL RESEARCH
CANCER METABOLISM

Received
25 September 2012

Accepted
11 March 2013

Published
25 March 2013

Correspondence and requests for materials should be addressed to T.N. (nisiyama@med.niigata-u.ac.jp)

Androgen deprivation promotes intratumoral synthesis of dihydrotestosterone from androgen metabolites in prostate cancer

Fumio Ishizaki[1], Tsutomu Nishiyama[1], Takashi Kawasaki[2], Yoshimichi Miyashiro[3], Noboru Hara[1], Itsuhiro Takizawa[1], Makoto Naito[4] & Kota Takahashi[1]

[1]Division of Urology, Department of Regenerative and Transplant Medicine, Graduate School of Medical and Dental Sciences, Niigata University, Niigata, Japan, [2]Department of Pathology, Niigata Cancer Center Hospital, Niigata, Japan, [3]Aska Pharma Medical, Co., Ltd., Kawasaki, Japan, [4]Division of Cellular and Molecular Pathology, Graduate School of Medical and Dental Sciences, Niigata University, Niigata, Japan.

Intratumoral synthesis of dihydrotestosterone (DHT) from precursors cannot completely explain the castration resistance of prostate cancer. We showed that DHT was intratumorally synthesized from the inactive androgen metabolites 5α-androstane-3α/β,17β-diol (3α/β-diol) in prostate cancer cells via different pathways in a concentration-dependent manner. Additionally, long-term culture in androgen-deprived media increased transcriptomic expression of 17β-hydroxysteroid dehydrogenase type 6 (HSD17B6), a key enzyme of oxidative 3α-HSD that catalyzes the conversion of 3α-diol to DHT in prostate cancer cells. Correspondingly, the score for HSD17B6 in tissues of 42 prostate cancer patients undergoing androgen deprivation therapy (ADT) was about 2-fold higher than that in tissues of 100 untreated individuals. In men receiving ADT, patients showing biochemical progression had a higher HSD17B6 score than those without progression. These results suggested that 3α/β-diol also represent potential precursors of DHT, and the back conversion of DHT from androgen derivatives can be a promising target for combination hormone therapy.

Androgen deprivation therapy (ADT) has been the therapeutic mainstay for metastatic prostate cancer, although the treatment effect is palliative in most cases. The majority of patients with advanced prostate cancer have an initial response to ADT; however, most patients develop castration-resistant prostate cancer (CRPC), which is characterized by disease advancement with increasing levels of prostate-specific antigen (PSA) and/or deterioration of symptoms despite anorchid testosterone (T) levels[1].

Several studies have shown that intratumoral concentrations of T and dihydrotestosterone (DHT) sufficiently activate AR (androgen receptor)-dependent transcriptiomes and are maintained in CRPC despite castration levels of plasma T[2–5]. In particular, dehydroepiandrosterone (DHEA) was the most common precursor of T/DHT in prostate cancer tissue after ADT[6–8]. Despite the recent clinical success of abiraterone acetate and other inhibitors of adrenal androgen synthesis in CRPC, the 3-year survival rate does not still reach 50% even with advanced ADT[9].

DHT is reduced by aldo-keto reductase 1C2 and 1C1 (AKR1C2 and AKR1C1) and is metabolized to 5α-androstane-3α,17β-diol (3α-diol) and 5α-androstane-3β,17β-diol (3β-diol), respectively[10–13] (Figure 1). Both 3α- and 3β-diol are unable to bind AR. Animal model studies have indicated an alternative pathway of DHT synthesis that utilizes 3α-diol as a precursor instead of T[14–16]. 3α-diol can be converted back to DHT via oxidative 3α-hydroxysteroid dehydrogenase (HSD) activity[17–20]. 17β-hydroxysteroid dehydrogenase type 6 (HSD17B6, known also as retinol dehydrogenase 3α-HSD) is the dominant or most potential enzyme in prostate tissue, associated with the back conversion of 3α-diol to DHT[21]. Chang et al. reported that the dominant route of DHT synthesis in CRPC bypasses T[22]. In this pathway, androstanedione and 3α-diol, not T, are precursors of DHT. On the other hand, the significance of the back conversion of 3α-diol to DHT in humans during ADT has barely been studied, despite evidence that the balance between DHT synthesis and metabolism determines intratumoral DHT concentrations[23]. Conversely, it has been reported that synthesis of DHT from 3β-diol is prevented because 3β-diol is either irreversibly hydroxylated at C-6 and/or C-7 positions or is oxidized to (epi) androsterone (ADT)[24–28]. It has

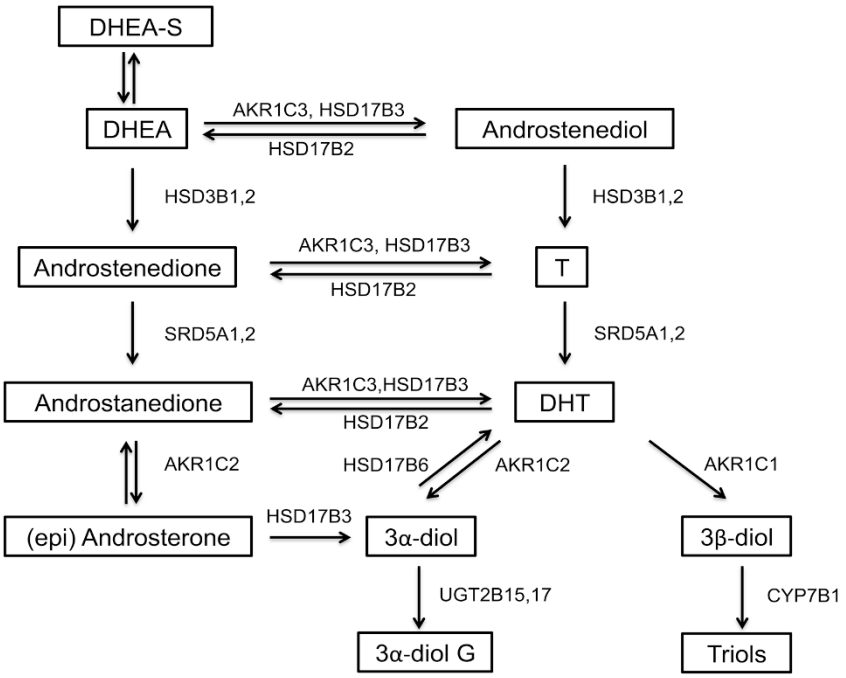

Figure 1 | C19 androgen metabolism pathway. C21 precursors (pregnenolone and progesterone) are converted to C19 adrenal androgens, such as dihydroepiandrosterone (DHEA) and androstenedione (A-dione) by the sequential hydroxylase and lyase activities of CYP17A1. Circulating adrenal androgens enter the prostate and can be converted to testosterone or androstanedione by a series of reactions involving the activity of HSD3B (3β-hydroxysteroid dehydrogenase), HSD17B (17β-hydroxysteroid dehydrogenase), and AKR1C (aldo-keto reductase) enzymes. Testosterone or androstanedione is then converted to the potent androgen DHT by the activity of SRD5A (steroid 5α-reductase). DHT is reduced by AKR1C2 and AKR1C1 to 5α-androstane-3α, 17β-diol (3α-diol) and 5α-androstane-3β, 17β-diol (3β-diol), respectively. 3α-diol is conjugated by UDP-glucronosyltransferases (UGT) enzymes such as UGT2B15 and UGT2B17 to 3α-diol glucuronide (3α-diol G). 3β-diol is hydroxylated by cytochrome P450-7B1 (CYP7B1) to triol.

been suggested that 3β-diol is a potent ligand for estrogen receptor β (ERβ). A few studies implied that ERβ signaling has potential as a suppressor in prostate growth and plays anti-proliferative and apoptotic roles in the prostate[29,30]. 3α-diol is conjugated by UDP-glucronosyltransferases (UGT) enzymes such as UGT2B15 and UGT2B17 to 3α-diol glucuronide (3α-diol G)[31], whereas 3β-diol is inactivated by metabolism to triols by CYP7B1 (cytochrome P450-7B1)[28]. However, no study has examined intracellular androgen synthesis from 3α-diol or 3β-diol with direct analysis and certification.

In the present study, we analyzed the intracellular androgen levels under incubation with the addition of 3α- or 3β-diol into prostate cancer cells using high-performance liquid chromatography tandem mass spectrometry (LC/MS). Additionally, we established an androgen deprivation model utilizing a hormonally-controlled long-term cell culture to examine whether or how HSD17B6 converts 3α-diol into DHT showed altered expression during ADT, highlighting the significance of 3α-diol in androgen metabolism in ordinary as well as androgen-deprived hormonal milieu. Moreover, we performed serological studies to denote the significance of circulating 3α-diol G levels.

Results

Androgenic activity of 3α- and 3β-diol and the production of DHT from 3α- and 3β-diol. PSA levels in media were increased by 3α-diol in a concentration-dependent manner both in LNCaP (Figure 2A) and VCaP cells (Figure 2B). Bicalutamide alone had no significant effect on PSA secretion in both cell lines without 3α- or 3β-diol (data not shown). In LNCaP cells pretreated with 100 nM 3α-diol, treatment with bicalutamide in negative controls, 0.1, 1, and 10 μM decreased PSA production in media (Figure 2C). In VCaP cells pretreated with 10 nM 3α-diol, treatment with bicalutamide in negative controls, 0.1, 1, and 10 μM decreased PSA production in media (Figure 2D). Similarly to 3α-diol, 3β-diol also increased PSA levels in media in a concentration-dependent manner both in LNCaP (Figure 2E) and VCaP cells (Figure 2F). In both LNCaP and VCaP cells respectively, pretreated with 1 nM 3β-diol, treatment with bicalutamide in negative controls, 0.01, 0.1, and 1 μM decreased PSA production in media (Figure 2G: LNCaP cells, Figure 2H: VCaP cells).

To show the intracellular effect of 3α- and 3β-diol, we concurrently measured the levels of DHEA, androstenediol (A-diol), androstenedione (A-dione), T, and DHT in LNCaP and VCaP cells treated with 3α- or 3β-diol and their respective culture media. Intracellular levels of DHEA, A-diol, A-dione, T, and DHT were detected in LNCaP cells pretreated with 1 nM, 10 nM, and 100 nM of 3α-diol (Figure 3A). Culture media levels of DHEA, A-diol, A-dione, T, and DHT were detected in LNCaP cells pretreated with 1 nM, 10 nM, and 100 nM of 3α-diol (Figure 3B). Intracellular levels of DHEA, A-diol, A-dione, T, and DHT were detected in VCaP cells pretreated with 1 nM, 10 nM, and 100 nM of 3α-diol (Figure 3C). Culture media levels of DHEA, A-diol, A-dione, T, and DHT were detected in VCaP cells pretreated with 1 nM, 10 nM, and 100 nM of 3α-diol (Figure 3D). Intracellular levels of DHEA, A-diol, A-dione, T, and DHT were detected in LNCaP cells pretreated with 1 nM, 10 nM, and 100 nM of 3β-diol (Figure 3E). Culture media levels of DHEA, A-diol, A-dione, T, and DHT were detected In LNCaP cells pretreated with 1 nM, 10 nM, and 100 nM of 3β-diol (Figure 3F). Intracellular levels of DHEA, A-diol, A-dione, T, and DHT were detected In VCaP cells pretreated with 1 nM, 10 nM, and 100 nM of 3β-diol (Figure 3G). Culture media levels of DHEA, A-diol, A-dione, T, and DHT were detected in VCaP cells pretreated with 1 nM, 10 nM and 100 nM of 3β-diol (Figure 3H).

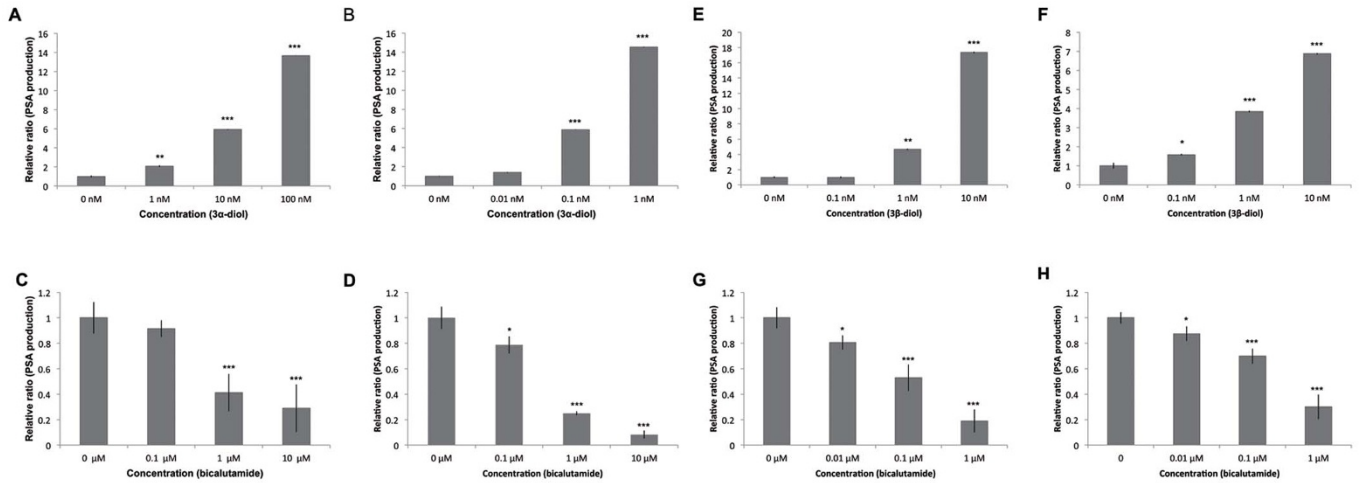

Figure 2 | Androgenic activity of 3α- and 3β-diol in LNCaP and VCaP cells. (A) Relative PSA levels in media in LNCaP cells (1×10^5 cells/ml) treated with 3α-diol (1, 10, and 100 nM) for 3 days. (B) Relative PSA levels in media in VCaP cells (1×10^5 cells/ml) treated with 3α-diol (0.01, 0.1, and 1 nM) for 3 days . (C) Relative PSA levels in media in LNCaP cells (1×10^5 cells/ml) treated with 3α-diol (100 nM) and/or bicalutamide (0.1, 1, and 10 μM) for 3 days. (D) Relative PSA levels in media in VCaP cells (1×10^5 cells/ml) treated with 3α-diol (10 nM) and/or bicalutamide (0.1, 1, and 10 μM) for 3 days. (E) Relative PSA levels in media in LNCaP cells (1×10^5 cells/ml) treated with 3β-diol (0.1, 1, and 10 nM) for 3 days. (F) Relative PSA levels in media in VCaP cells (1×10^5 cells/ml) treated with 3β-diol (0.1 nM, 1 nM, and 10 nM) for 3 days. (G) PSA levels in media in LNCaP cells (1×10^5 cells/ml) treated with 3β-diol (1 nM) and/or bicalutamide (0.01, 0.1, and 1 μM) for 3 days. (H) Relative PSA levels in media in VCaP cells (1×10^5 cells/ml) treated with 3β-diol (1 nM) and/or bicalutamide (0.01, 0.1, and 1 μM) for 3 days. PSA levels in media in LNCaP and VCaP cells were increased by 3α- or 3β-diol alone in a concentration-dependent manner. PSA levels in media in LNCaP and VCaP cells pretreated with 3α- or 3β-diol showed a dose-dependent decrease in PSA production when bicalutamide was added at various concentrations. Data are means ± s.d and are representative of at least three independent experiments. PSA levels in media in LNCaP and VCaP cells pretreated with 3α- or 3β-diol showed a dose-dependent decrease in PSA production when bicalutamide was added at various concentrations. Data are means ± s.d and are representative of at least three independent experiments. * $P < 0.05$, ** $P < 0.01$, *** $P < 0.001$ by multiple comparisons using a one-way ANOVA and Turkey's post hoc test.

Increased HSD17B6 expression detected by RT-PCR and immunohistochemistry and inhibition of HSD17B6 expression by siRNA. In DHEA-treated LNCaP cells at lower passage numbers (22 passages or less), transcriptome expression of HSD17B6 and 17β-hydroxysteroid dehydrogenase type 4 (HSD17B4), which also has 3α- HSD oxidase activity, showed far less changes (Figure 4A) than in cells at higher passage numbers (32 passages or more), where HSD17B6 mRNA expression was up-regulated (Figure 4B). HSD17B6 expression in cells at passages greater than 32 was more than 2-fold higher than cells at 4 passages. On the other hand,

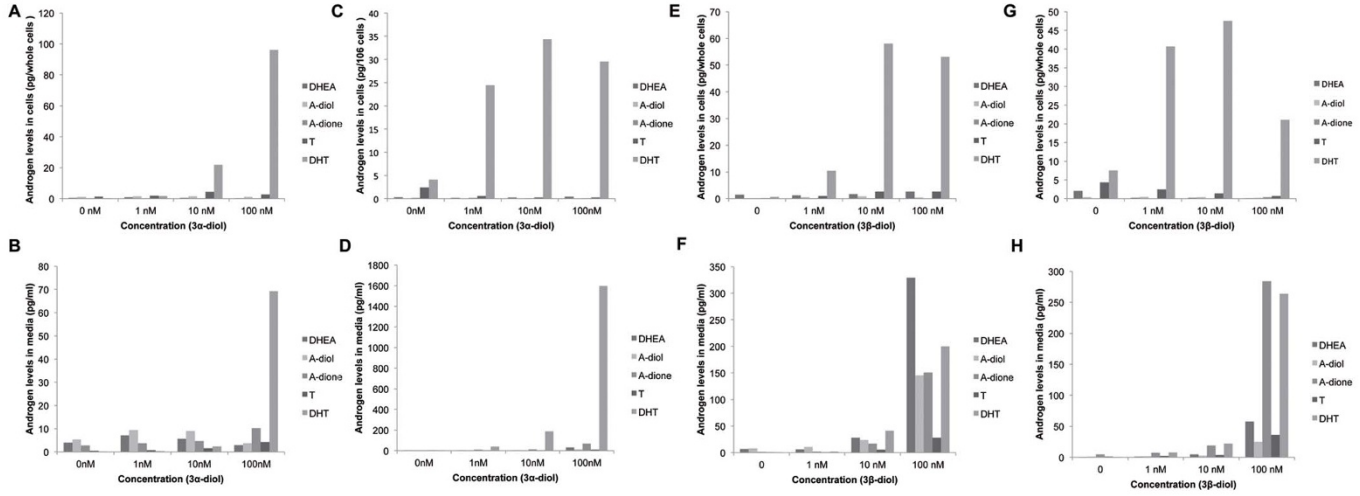

Figure 3 | Production of C19 androgens from 3α- and 3β-diol in LNCaP and VCaP cells. Intracellular levels of DHEA, A-diol, A-dione, T, and DHT in LNCaP and VCaP cells treated with 3α- or 3β-diol. After 1×10^6 LNCaP and VCaP cells (for VCaP cells in 3β-diol experiments, cells were 2×10^6 cells) were cultured in the presence or absence of 1, 10, and 100 nM of 3α- or 3β-diol for 3 days, cells were collected and intracellular androgen levels were measured. Androgen levels were indicated as 'pg/whole cells'. Androgen levels in media were indicated as 'pg/ml'. (A) Production of DHEA, A-diol, A-dione, T, and DHT from 3α-diol in LNCaP cells. (B) Production of DHEA, A-diol, A-dione, T, and DHT from 3α-diol in media used to culture LNCaP cells. (C) Production of DHEA, A-diol, A-dione, T, and DHT from 3α-diol in VCaP cells. (D) Production of DHEA, A-diol, A-dione, T, and DHT from 3α-diol in media used to culture VCaP cells. (E) Production of DHEA, A-diol, A-dione, T, and DHT from 3β-diol in LNCaP cells. (F) Production of DHEA, A-diol, A-dione, T, and DHT from 3β-diol in media used to culture LNCaP cells. (G) Production of DHEA, A-diol, A-dione, T, and DHT from 3β-diol in VCaP cells. (H) Production of DHEA, A-diol, A-dione, T, and DHT from 3β-diol in media used to culture VCaP cells.

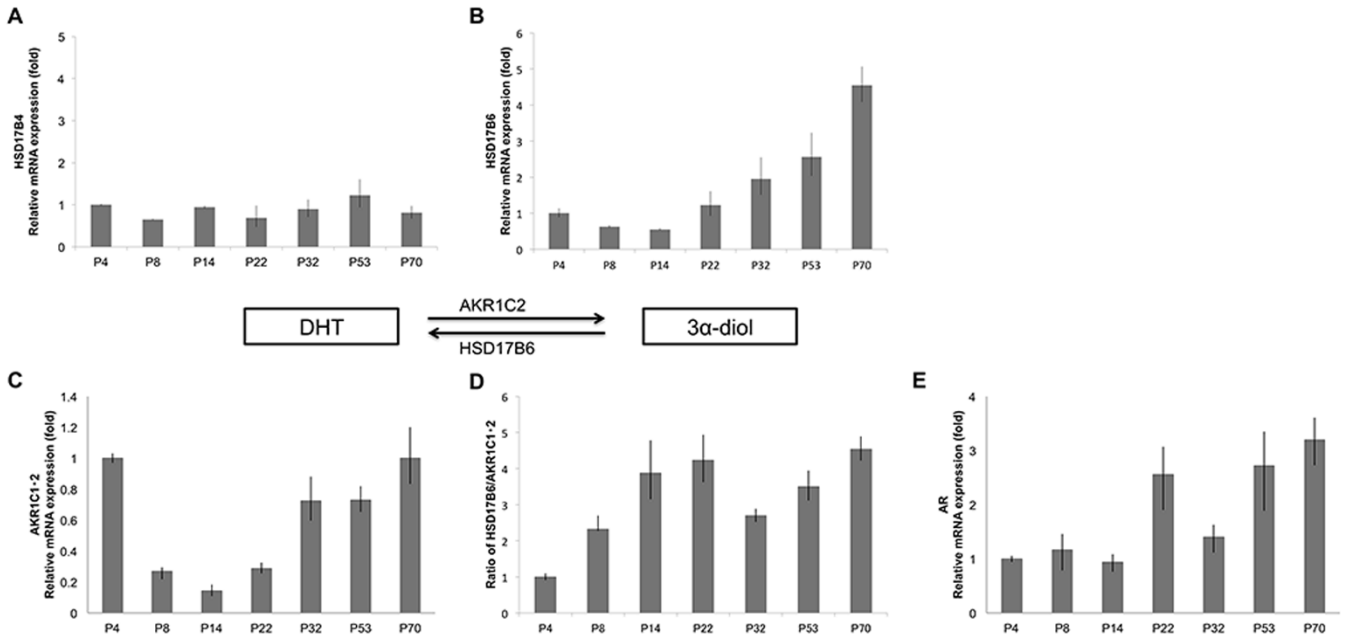

Figure 4 | Changes in HSD17B4, HSD17B6, and AKR1C1·2 gene expression in LNCaP cells treated with 1 nM DHEA hormone-depleted medium. Transcriptome expression of HSD17B4, HSD17B6, and AKR1C1·2 in LNCaP cells cultured continuously in steroid hormone-depleted medium with 1 nM DHEA were analyzed by RT-PCR. Results are expressed as fold changes relative to the value obtained in LNCaP cells passaged 4 times. (A) HSD17B4 mRNA expression relative to the value obtained in cells passaged 4 times. (B) HSD17B6 mRNA expression relative to the value obtained in cells passaged 4 times. (C) AKR1C1·2 mRNA expression relative to the value obtained in cells passaged 4 times. (D) Ratio of HSD17B6/AKR1C1·2 relative to the value obtained in cells passaged 4 times. (E) AR mRNA expression relative to the value obtained in cells passaged 4 times. P indicates passage number.

AKR1C1·2, which reduced DHT to 3β and 3α-diol, was down-regulated at the beginning of androgen deprivation (Figure 4C). The ratio of HSD17B6/AKR1C1·2 transcriptome expression increased with time (Figure 4D).

Both HSD17B4 and HSD17B6 were expressed in the cytoplasm of carcinoma cells (Figure 5A); HSD17B4 exhibited a granular pattern. Neither a nuclear nor membranous pattern for both HSD17B4 and HSD17B6 was observed. In the non-neoplastic peripheral zone, immunoreactivity for HSD17B4 and HSD17B6 was detected in both acinar and basal cells. Expression scores for HSD17B4 and HSD17B6 in those who did not receive ADT (non-ADT group) were 158.9 ± 83.8 and 71.9 ± 64.9, respectively. Expression scores for HSD17B4 and HSD17B6 in those who received ADT (ADT group) were 136.9 ± 66.3 and 143.6 ± 76.3, respectively. The score for HSD17B6 in the ADT group was about 2-fold higher than that in the non-ADT group ($P < 0.001$) (Figure 5B, Table 1). In contrast, there was no significant difference in the expression of HSD17B4 between ADT and non-ADT groups ($P = 0.134$). In a comparison of ADT patients with and without biochemical progression, the biochemical progression group had a significantly higher score of HSD17B6 than the biochemical progression-free group ($P = 0.038$); however, there were no significant differences in HSD17B4 scores between the two groups ($P = 0.650$) (Figure 5C, Table 2). In addition, the score for HSD17B6 in the ADT group significantly correlated with ADT duration ($rs = 0.451$, $P = 0.003$). There was no significant relationship between the score for both HSD17B4 and HSD17B6 and the Gleason score or PSA levels.

To confirm the role of HSD17B6 in the metabolism of 3α-diol, we used HSD17B6 siRNA to interfere with HSD17B6 expression in LNCaP cells. Transfection with HSD17B6 siRNA significantly reduced PSA by 20.6% in long-term androgen depleted LNCaP cells treated with 3α-diol ($P = 0.014$) (Figure 5D).

Correlation between serum 3α-diol G levels and other parameters before and after ADT. Of the 72 patients, 28 (39%) discontinued flutamide treatment because of adverse effects: 24 patients due to an increase in transaminase levels, and 4 because of diarrhea. When transaminase levels of patients increased, we immediately discontinued flutamide in order to prevent severe liver dysfunction. Transaminase levels recovered within 4 weeks, and diarrhea disappeared immediately after the discontinuation of flutamide. All 28 patients received gonadotropin-releasing hormone (GnRH) agonist monotherapy for the remaining treatment period. Comparisons of analytical values before and after ADT are presented in Table 3. Correlations between serum 3α-diol G levels and androgens or related hormones before and after ADT are presented in Table 4. Before ADT, 3α-diol G levels correlated with serum DHEA-S (dehydroepiandrosterone sulfate) ($P = 0.001$, Figure 6A), and androstenedione (A-dione) ($P = 0.049$). After ADT, serum 3α-diol G levels correlated with serum DHEA-S ($P < 0.001$, Figure 6B), A-dione ($P < 0.001$), T ($P < 0.001$), and PSA levels ($P = 0.006$).

Discussion

Our study has three major findings. First, intracellular DHT is synthesized from inactive androgen 3α- and 3β-diol via different pathways in prostate cancer cells. This is the first report to reveal that 3β-diol can be a precursor of DHT in prostate cancer cells. Second, prolonged androgen deprivation increased transcriptomic expression of HSD17B6 in LNCaP cells, and the expression score of HSD17B6 in prostate cancer tissues treated with ADT was also significantly higher than in those who did not receive ADT. In a comparison of ADT patient groups with and without biochemical progression, the biochemical progression group had a significantly higher score of HSD17B6 than the biochemical progression-free group. Finally, serum 3α-diol G levels reflect the androgen milieu in localized prostate cancer patients receiving ADT.

Intracellular and medium androgen levels under incubation with the addition of 3α- or 3β-diol into LNCaP and VCaP cells measured by the detailed LC/MS method indicated that 3α-diol was directly

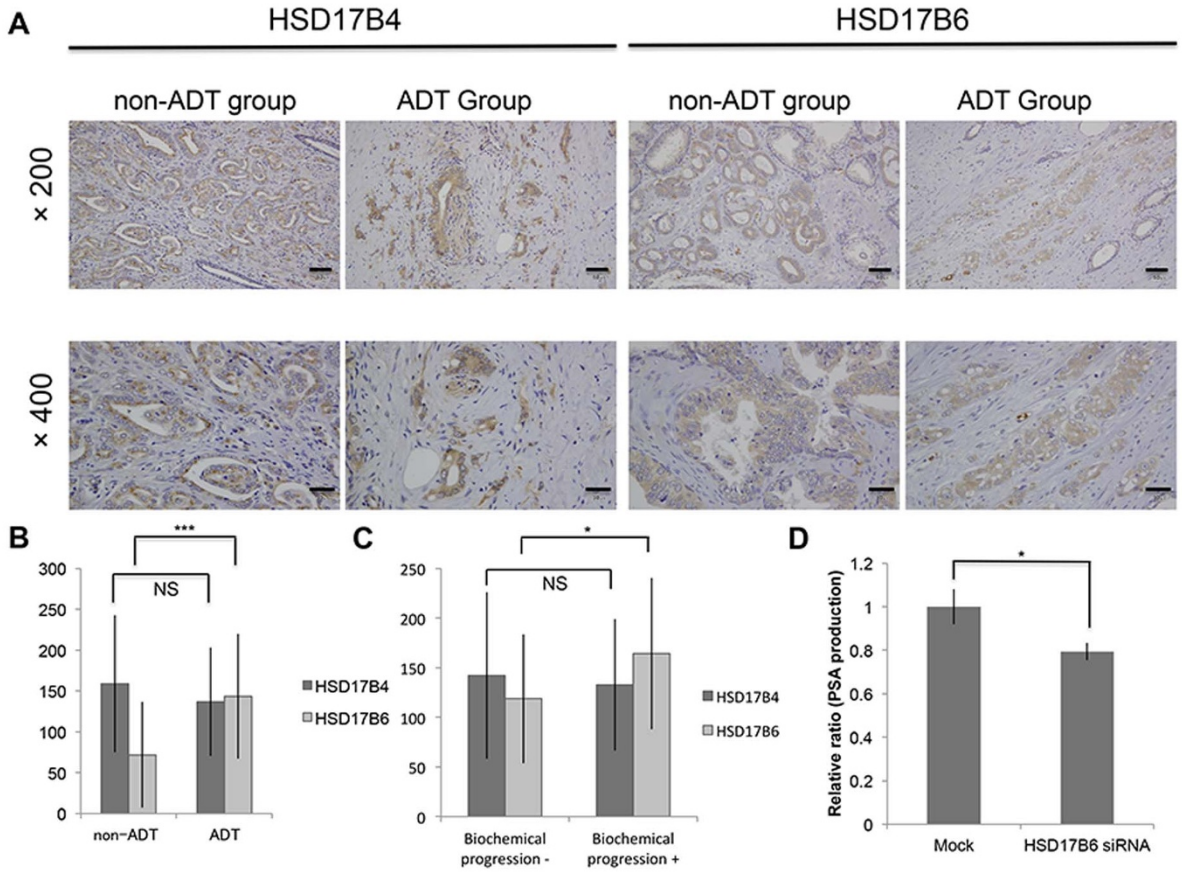

Figure 5 | Immunohistochemical expression of HSD17B4 and HSD17B6 in prostate cancer tissues and inhibition of HSD17B6 expression by siRNA. (A) Both HSD17B4 and HSD17B6 were expressed in the cytoplasm of carcinoma cells. The cytoplasmic staining pattern for HSD17B4 had a granular pattern. Neither a nuclear nor membranous pattern for both HSD17B4 and HSD17B6 was observed. Top scale bar, 50 μm; bottom scale bar 30 μm. (B) The score for HSD17B6 in the ADT group was about 2-fold higher than that without ADT ($P < 0.001$). In contrast, there were no significant differences in the expression of HSD17B4 between those with and without ADT ($P = 0.134$). (C) In a comparison between ADT patient groups with and without biochemical progression, the former group had a significantly higher score of HSD17B6 than the latter ($P = 0.038$). (D) The HSD17B6 gene was silenced in 49 passaged hormonally controlled androgen deprivation LNCaP cells. HSD17B6-transfected cells and control-transfected cells treated with (1 nM) 3α-diol were cultured for 3 days. PSA production in HSD17B6-transfected cells was significantly lower than that in control-transfected cells ($P = 0.014$). Each experiment was performed in triplicate. Data are means ± s.d. and are representative of at least three independent experiments. * $P < 0.05$, ** $P < 0.01$, *** $P < 0.001$, NS, not significant by the Student's t test.

converted to DHT in prostate cancer cells. The large difference in conversion of 3a-diol to DHT in VCaP versus LNCaP cells indicated that VCaP cells convert from 3a-diol to DHT more effectively than LNCaP cells do. However, VCaP cells respond lower to androgens about cell growth than LNCaP cells (data not shown). VCaP cells may need larger amount of androgens about cell growth than LNCaP cells. On the other hand, although it has been reported that the direct formation of DHT from 3β-diol is virtually irreversible, our studies showed the synthesis of DHT from 3β-diol in both prostate cancer cell lines and culture medium. Different from the results of 3α-diol, we found a lot of other C19 androgens such as A-dione, A-diol, and DHEA in prostate cancer cells and the culture medium. Synthesis of T is low relative to A-dione, A-diol, and DHEA. These results suggest that synthesis of DHT from 3β-diol is different from the direct conversion from 3α-diol to DHT. It suggested that 3β-diol may firstly be

Table 1 | Characteristics of patients receiving radical prostatectomy

	Non-ADT group (n = 100)	ADT group (n = 42)	*P* value
Mean age (years)	63.4 ± 6.5	64.8 ± 6.0	0.229
PSA (ng/ml)	9.2 ± 8.2	20.3 ± 16.7	<0.001
Gleason score			0.182
5–6	37	11	
7	38	23	
=>8	25	8	
HSD17B4 score	158.9 ± 83.8	136.9 ± 66.3	0.134
HSD17B6 score	71.9 ± 64.9	143.6 ± 76.3	<0.001

Table 2 | Comparison of ADT patients with and without biochemical progression

	Biochemical progression − (n = 19)	Biochemical progression + (n = 23)	*P* value
Mean age (years)	66.1 ± 5.2	63.4 ± 6.6	0.223
PSA (ng/ml)	15.6 ± 17.6	23.3 ± 15.3	0.131
Gleason score			0.247
=<6	8	3	
7	9	14	
=>8	2	6	
ADT duration	6.6 ± 2.1	10.1 ± 10.1	0.173
HSD17B4 score	142.1 ± 74.7	132.6 ± 59.9	0.650
HSD17B6 score	118.7 ± 64.2	164.1 ± 71.6	0.038

Table 3 | Comparison of 3α-diol G, PSA, androgens, and related hormones before and after ADT

	Before ADT Mean (SD)	After ADT Mean (SD)	*P* value
T (ng/ml)	4.62 (0.15)	0.15 (0.10)	<0.001
DHT (ng/ml)	0.88 (0.41)	0.05 (0.12)	<0.001
DHEA-S (μg/dl)	133.3 (63.8)	83.4 (51.4)	<0.001
A-dione (ng/dl)	160.5 (60.2)	80.2 (40.1)	<0.001
3α-diol G (ng/ml)	3.5 (2.0)	1.0 (0.9)	<0.001
PSA (ng/ml)	17.9 (14.0)	0.20 (0.35)	<0.001

Table 4 | Correlations between serum 3α-diol G levels and androgens or related hormones before and after ADT

	Before ADT		After ADT	
	rs. by 3α-diol G	*P* value	rs. by 3α-diol G	*P* value
T	0.019	0.878	0.460	<0.001
DHT	−0.046	0.717	0.224	0.060
DHEA-S	0.385	0.001	0.558	<0.001
A-dione	0.244	0.049	0.470	<0.001
PSA	0.028	0.824	0.321	0.006

converted to epi-ADT, then epi-ADT may be converted to androstanedione, which, in turn, may be converted to DHT. Excess androstanedione may be stored in DHEA or A-diol. Briefly, synthesis of DHT from 3α- or 3β-diol utilizes different pathways. This is the first study to indicate that 3β-diol is the potential precursor of DHT in prostate cancer cells using the detailed LC/MS method. These results partly explained the fact that finasteride, a 5α-reductase type 2 inhibitor, or dutasteride, a dual 5α-reductase type 1 and 2 inhibitor, were ineffective in preventing prostate cancer development[32,33] or in treating CRPC patients[34,35].

A few studies reported that 3β-diol is a potential ligand of estrogen receptor β (ERβ) and has an antiproliferative effect. However, our results revealed that 3β-diol is potentially a precursor of DHT in prostate cancer cells. This reformation pathway from 3β-diol to DHT via epi-ADT and A-dione suggested that C19 androgens circled centering on DHT, and all C19 androgens may be a potential precursor of DHT. Broad pre-receptor regulation of AR may exist in prostate cancer cells. These results may help explain the mechanism of resistance to testosterone depletion.

Bauman et al. showed that 3α-diol is inactive at AR, but induces prostate growth, suggesting that oxidative 3α-HSD is present, and the main oxidative 3α-HSD in normal human prostate is RL-HSD (known as HSD17B6) and may be a new therapeutic target for treating prostate diseases[21]. We established the long-term androgen depleted LNCaP model treated with a physiological concentration of 1 nM DHEA. In the beginning of ADT, despite unchanged expression of HSD17B4 and HSD17B6, AKR1C1·2 ,which reduced DHT to its metabolite, was markedly reduced. Prostate cancer cells regulated DHT loss at the beginning of ADT. Then, transcriptome expression of HSD17B6 increased with time. Prostate cancer cells promoted synthesis from the DHT metabolite 3α-diol during the long duration of ADT.

To determine whether increased HSD17B6 mRNA expression was reflected in protein expression, we next assessed HSD17B6 protein by immunohistochemistry in radical prostatectomy specimens; expression of HSD17B6 protein in prostate cancer tissues receiving ADT has not previously been examined to our knowledge. The expression score of HSD17B6 in prostate cancer patients treated with ADT was significantly higher than those who had not received ADT. The score for HSD17B6 in the ADT group was significantly correlated with ADT duration ($rs = 0.451$, $P = 0.003$). These immunohistochemistry results correspond with transcriptome expression analyses. Comparison of patients with and without biochemical progression in the ADT group revealed that the biochemical progression group had a significantly higher HSD17B6 score. The expression of HSD17B6 in prostate cancer tissues can increase under low androgen milieu. Prostate cancer can produce DHT from not only the adrenal precursors but also reduced metabolites 3α-diol more autonomously under low androgen milieu. Prostate cancer with high HSD17B6 expression tends to progress biochemically. These results suggested that HSD17B6 is a potential therapeutic target. Next, we performed knockdown of HSD17B6 using androgen deprivation model LNCaP cells. HSD17B6 siRNA introduced into cells decreased PSA production under incubation with the addition of 3α-diol in LNCaP cells. These results showed that HSD17B6 has oxidative 3α-HSD activity, and plays a critical role in converting 3α-diol to DHT. Relatively low reductions in PSA levels are due to the contributions of other enzymes that have oxidative 3α-HSD activity.

We prospectively analyzed blood samples of 72 patients receiving ADT to reveal the in vivo kinetics of 3α-diol. We revealed that, before ADT, serum 3α-diol G levels correlated with serum DHEA-S and A-dione levels. After ADT, serum 3α-diol G levels correlated with serum DHEA-S, A-dione, T, and PSA levels. Correlations between serum 3α-diol G levels and adrenal androgens (DHEA-S, A-dione) were increased by a much larger extent. Serum 3α-diol G levels reflect the androgen milieu in localized prostate cancer patients; therefore, 3α-diol is not only a metabolite of DHT but also a potential precursor of DHT in prostate cancer. Correlations between serum 3α-diol G levels and adrenal androgens may reveal pre-receptor regulation of DHT using C19 androgen pool in the prostate cancer.

The advent of new drugs such as abiraterone acetate and TOK-001 that block CYP17A1 (Cytochrome P450 17α-hydroxylase and 17, 20 lyase) activity open the door to an advanced androgen deprivation approach since the novel report of Huggins and Hodges[36,37]. In a phase III trial of abiraterone acetate plus prednisone versus a placebo plus prednisone in CRPC patients previously treated with docetaxel, overall survival was 3.9 months longer in the abiraterone acetate-prednisone group[9]. Abiraterone acetate was approved by the US Food and Drug Administration in April 2011 for the treatment of metastatic CRPC patients. In the future, a large population of men may make the transition to abiraterone acetate-resistant CRPC. Therefore, understanding the mechanism of abiraterone acetate-resistant CRPC is a matter of overriding concern. The expression of PSA, which is under the control of the AR, implies that progression while on abiraterone acetate is related to the ongoing activity of the AR. Abiraterone acetate-resistant CRPC may be related a C19 androgen network in prostate cancer cells. Our study suggested that the intracellular C19 androgen network is a potential therapeutic target in abiraterone acetate-resistant CRPC.

In conclusion, we verified the synthesis of DHT from 3α- or 3β-diol via different pathways in prostate cancer cells in this study. We revealed that HSD17B6 expression levels in prostate cancer can be useful for the diagnosis of high-risk prostate cancer. We elucidated that serum 3α-diol G levels reflect the adrenal androgen milieu in localized prostate cancer patients. Our study revealed that 3α- and 3β-diol has a much more significant role in intratumoral androgen metabolism during ADT than previously thought, and the back conversion of DHT from 3α- and 3β-diol can be a promising target for advanced combination hormone therapy.

Methods

Cell lines and drugs. Human prostate cancer cell lines LNCaP and VCaP were purchased from the American Type Culture Collection (ATCC). LNCaP cells had mutated AR, and VCaP cells had wild-type AR[38,39]. 3α-diol and DHEA were purchased from Sigma Chemicals (St Louis, MO, USA). 3β-diol was purchased from Atomax Chemicals Co. (Shenzhen, China). Bicalutamide, an antagonist against AR, was purchased from Tocris Bioscience (Bristol, UK).

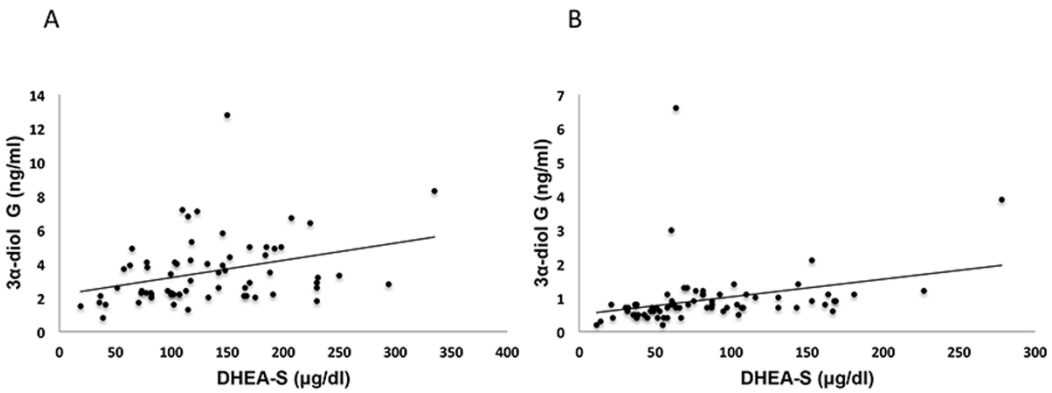

Figure 6 | Relationships between serum 3α-diol G and DHEA-S levels before and after ADT. Serum 3α-diol G levels were significantly correlated with serum DHEA-S levels before (A) and after (B) ADT (before ADT rs: 0.385, $P = 0.001$, after ADT rs: 0.558, $P < 0.001$).

Cell culture and drug treatment. Cells were cultured in RPMI 1640 (Gibco Invitrogen, Grand Island, NY, USA) supplemented with 10% heat-inactivated fetal bovine serum (FBS), 1% MEM nonessential amino acids, 1% MEM sodium pyruvate solution 100 mM, 0.14% $NaHCO_3$, and 80 mg/L of kanamycin, at 37°C in a humidified, 5% CO_2 atmosphere. Cells were grown to sub-confluence and switched to steroid hormone-depleted medium without phenol-red, containing 10% charcoal-dextran stripped FBS (Biowest, Paris, France), and were exposed to 3α-diol or 3β-diol and/or bicalutamide at various concentrations for three days. For Tandem-R PSA tests (Beckman Coulter Inc., San Diego, CA, USA), cells were plated at a density of 1×10^5 cells/ml in triplicate. To determine intracellular levels of DHEA, A-diol, A-dione, T, and DHT, LNCaP and VCaP cells were cultured in $75cm^3$ cell culture flasks with 10 ml medium at a concentration of 1×10^5 cells/ml (for VCaP cells in 3β-diol experiments, the concentration was 2×10^5 cells/ml) in the presence or absence of 1, 10, and 100 nM of 3α- or 3β-diol for three days. Androgen levels in cells collected from cell culture flasks were indicated as 'pg/whole cells', while androgen levels in medium collected from cell culture flasks were indicated as 'pg/ml'.

LNCaP cells were cultured continuously in steroid hormone-depleted medium without phenol-red, containing 10% charcoal-dextran stripped FBS with a physiological concentration of 1 nM DHEA. LNCaP cells were passaged once every 5 days. Analyses of transcriptome expression were performed at 4, 8, 14, 22, 32, 53, and 70 passages.

LC-MS/MS analysis. DHEA, A-diol, A-dione, T, and DHT concentrations in cells and media were determined as described previously[40]. In brief, cells were homogenized in distilled water. Steroids in homogenized cells and media were respectively extracted with ethyl acetate, and then, extracts were purified using a solid phase extraction cartridge. After derivatization to picolinate ester forms, concentrations of steroids were determined with LC-MS/MS. The limits of quantification of DHEA, A-diol, A-dione, T, and DHT were 2, 1, 2, 1, and 1 pg, respectively.

RNA extraction and real-time PCR. Total RNA was isolated from LNCaP cells treated with 1 nM DHEA according to the RNAqueous®-4PCR Kit protocol (Ambion, Austin, TX, USA). cDNA was generated using the High-Capacity cDNA Reverse Transcription Kit (Applied Biosystems, Foster City, CA, USA) according to the manufacturer's instructions. Incubation conditions were as follows: 10 min at 25°C and 2 h at 37°C. Real-time PCR (RT-PCR) experiments were carried out using a standard TaqMan PCR protocol according to the manufacturer's recommendations (Applied Biosystems). Transcripts of the housekeeping gene, β-actin (ACTB), were measured as the internal control. Assays were carried out using the ABI 7500 Real Time PCR system and Taqman Gene Expression assay mix (Applied Biosystems; Assay ID: Hs00264973_m1 for HSD17B4, Hs00366258_m1 for HSD17B6, Hs00413886_m1 for AKR1C1·2, Hs00171172_m1 for AR, and Hs99999903_m1 for ACTB). PCRs were carried out after incubation at 50°C for 2 minutes and denaturing at 95°C for 10 minutes, followed by 40 cycles at 95°C for 15 seconds and 60°C for 1 minute. Quantification of target gene expression in samples was accomplished by measuring the fractional cycle number at which the amount of expression reached a fixed threshold (CT). Relative quantification was given by CT values, determined by triplicate reactions. Triplicate CT values were averaged and ACTB CT was subtracted to obtain ΔCT. ΔΔCT was then calculated by subtracting ΔCT of the control (4 passages) from ΔCT of the sample. Relative expression levels were determined as $2^{-\Delta\Delta CT}$.

Immunohistochemistry. Prostate tissue was obtained from 142 patients who had undergone radical prostatectomy at Niigata University and Niigata Cancer Center Hospital between 1999 and 2006. One hundred patients had undergone radical prostatectomy without prior therapy (non-ADT group). Forty-two patients had undergone radical prostatectomy with neoadjuvant ADT (ADT group). The mean duration of ADT was 8.4 months (median, 6.8 months). ADT was discontinued after radical prostatectomy. Patients receiving ADT showed higher PSA levels ($P < 0.001$). Gleason scores and ages did not differ between non-ADT and ADT groups (Table 1). Biochemical progression after radical prostatectomy was defined as two consecutive PSA values of 0.2 ng/ml or greater at any time post-operatively or any additional treatment more than 6 months after radical prostatectomy. The procedure for this research project was approved by the Ethics Committees of our institutions. Informed consent was obtained from all patients.

Rabbit polyclonal antibody for HSD17B4 was obtained from GeneTex (Irvine, CA, USA), and rabbit polyclonal antibody for HSD17B6 was obtained from Abcam (Cambridge, MA, USA)[41,42]. Both anti-HSD17B4 and HSD17B6 antibodies were used for immunohistochemistry at 8 μg/ml. Immunohistochemistry methods were performed as described previously[43]. All slides were assessed by a urological pathologist (T.K.). Immunoreactivity was scored based on our previous report[43]. In brief, the extent of protein expression was scored semi-quantitatively by a combination of the staining intensity and fraction of positive cells in the tumor area. Intensity was graded as follows: 0, no detectable signal; 1, weak signal at intermediate to high power fields; 2, moderate signal at low to intermediate power fields; 3, strong signal at low power field. The score was calculated by summing each staining intensity and multiplying by the percentage of positive cells.

Transfection via electroporation. 1 nM DHEA-treated LNCaP cells in steroid hormone-depleted medium without phenol-red, containing 10% charcoal-dextran stripped FBS (passage number: 49 times) were prepared for transfection. Five $\times 10^5$ LNCaP cells were resuspended in 100 μl resuspension buffer R (Neon Transfection System; Invitrogen, Carlsbad, CA, USA) with 5 μM siRNA for HSD17B6 (s225011; Ambion) or control non-silencing siRNA (#1 siRNA; Ambion) and transfected in 100 μl Neon tip with Neon transfection system (Invitrogen) using two pulses (1100 V input pulse voltage/20 ms input pulse width). Transfected HSD17B6 were plated at a concentration of 1×10^5 cells/ml per 25 cm^2 flasks in triplicate and were cultured in phenol-red free medium with 10% charcoal–dextran stripped of FBS with 1 nM 3α-diol for 3 days before Tandem- R PSA tests.

Patients and blood sampling. Patients who had received any prior treatment for prostate cancer were excluded. In total, 72 consecutive patients who were treated with radiotherapy for localized or locally advanced prostate cancer (cT1c–3a N0 M0) at the Department of Urology, Niigata University Hospital, were enrolled between May 2004 and December 2006. The study was prospectively designed, and the procedure for this research project was approved by the Ethics Committee of our institution . Informed consent was obtained from all patients. Mean patient age at diagnosis was 69.0 years (range 54 to 79). Mean PSA at diagnosis was 17.9 ng/ml (range 5.2 to 100.9) and the mean Gleason score was 7.2 (range 5 to 9). Patients received a subcutaneous injection of a GnRH agonist, goserelin acetate (3.6 mg, every 4 weeks), and peroral non-steroidal anti-androgen flutamide (375 mg/day) for 6 months, prior to radiotherapy. Flutamide treatment was discontinued in 28 of 72 patients because of adverse effects: at 1 month, 6 patients; at 2 months, 4 patients; at 3 months, 8 patients; at 4 months, 4 patients; and at 5 months, 6 patients. Elevations in serum transaminase levels and diarrhea were the causes of discontinuation in 24 and 4 patients, respectively. To prevent severe liver dysfunction, the administration of flutamide was immediately discontinued when elevated serum transaminase levels were noted. Transaminase levels recovered within 4 weeks, and diarrhea disappeared immediately after the discontinuation of flutamide. All 28 patients received GnRH agonist monotherapy for the remaining treatment period. Hormonal parameters were quantified by SRL Laboratory (Tokyo, Japan). PSA (Beckman Coulter Inc., San Diego, CA, USA), and T (ECLusys Testosterone Kit, Roche Diagnostics, Indianapolis, IN, USA) were determined by an electrochemiluminescence immunoassay (ECLIA). DHT, A-dione (DPC androstenedione Kit, Mitsubishi Kagaku Iatron, Inc., Tokyo, Japan,) and 3α-diol G (Androstanediol Glucronide RIA, Diagnostic Systems

Laboratories, Inc., Webster, TX, USA, intra-assay CV: 4.5–10.0%, inter-assay CV: 4.2–7.6%) were measured by radioimmunoassay (RIA). DHEA-S was quantified using the chemiluminescent enzyme immunoassay (CLEIA Access DHEA-S, Beckman Coulter, Inc., Fullerton, CA, USA, intra-assay CV: 5.53–6.46%, inter-assay CV: 2.67–7.71%).

Data analysis and Statistical methods. Differences between experimental groups were analyzed by the Student's t, chi-square, and Fisher's exact tests. Pearson's correlation coefficients were used to assess the relationship between experimental variables. The Wilcoxon signed-rank test was used to compare changes in paired parameters before and after ADT. Correlations between 3α-diol G level androgens, related hormones, and PSA before and after ADT were analyzed using Spearman's rank correlation coefficient analysis. We performed multiple comparisons using a one-way ANOVA and Turkey's post hoc test. The test was two-sided and $P < 0.05$ was considered significant. All analyses were performed using SPSS version 15.0J (SPSS Inc., Chicago, IL, USA) on a Windows-based computer.

1. Oh, W. K. & Kantoff, P. W. Management of hormone refractory prostate cancer: current standards and future prospects. *J Urol.* **160**, 1220–1229 (1998).
2. Page, S. T. *et al.* Persistent intraprostatic androgen concentrations after medical castration in healthy men. *J Clin Endocrinol Metab.* **91**, 3850–3856 (2006).
3. Mohler, J. L. *et al.* The androgen axis in recurrent prostate cancer. *Clin Cancer Res.* **10**, 440–448 (2004).
4. Titus, M. A. *et al.* Testosterone and dihydrotestosterone tissue levels in recurrent prostate cancer. *Clin Cancer Res.* **11**, 4653–4657 (2005).
5. Montgomery, R. B. *et al.* Maintenance of intratumoral androgens in metastatic prostate cancer: a mechanism for castration-resistant tumor growth. *Cancer Res.* **68**, 4447–4454 (2008).
6. Nishiyama, T. *et al.* The influence of androgen deprivation therapy on dihydrotestosterone levels in the prostatic tissue of patients with prostate cancer. *Clin Cancer Res.* **10**, 7121–7126 (2004).
7. Geller, J. Rationale for blockade of adrenal as well as testicular androgens in the treatment of advanced prostate cancer. *Semin Oncol.* **12**, 28–35 (1985).
8. Labrie, F. Adrenal androgens and intracrinology. *Semin Reprod Med.* **22**, 299–309 (2004).
9. de Bono, J. S. *et al.* Abiraterone and increased survival in metastatic prostate cancer. *N Engl J Med.* **364**, 1995–2005 (2011).
10. Steckelbroeck, S. *et al.* Human cytosolic 3alpha-hydroxysteroid dehydrogenases of the aldo-keto reductase superfamily display significant 3beta-hydroxysteroid dehydrogenase activity: implications for steroid hormone metabolism and action. *J Biol Chem.* **279**, 10784–10795 (2004).
11. Bauman, D. R. *et al.* Transcript profiling of the androgen signal in normal prostate, benign prostatic hyperplasia, and prostate cancer. *Endocrinology.* **147**, 5806–5816 (2006).
12. Jin, Y. & Penning, T. M. Multiple steps determine the overall rate of the reduction of 5alpha-dihydrotestosterone catalyzed by human type 3 3alpha-hydroxysteroid dehydrogenase: implications for the elimination of androgens. *Biochemistry.* **45**, 13054–13063 (2006).
13. Rizner, T. L. *et al.* Human type 3 3alpha-hydroxysteroid dehydrogenase (aldo-keto reductase 1C2) and androgen metabolism in prostate cells. *Endocrinology.* **144**, 2922–2932 (2003).
14. Walsh, P. C. & Wilson, J. D. The induction of prostatic hypertrophy in the dog with androstanediol. *J Clin Invest.* **57**, 1093–1097 (1976).
15. Shaw, G. *et al.* Role of the alternate pathway of dihydrotestosterone formation in virilization of the Wolffian ducts of the tammar wallaby, Macropus eugenii. *Endocrinology.* **147**, 2368–2373 (2006).
16. Shaw, G. *et al.* Prostate formation in a marsupial is mediated by the testicular androgen 5 alpha-androstane-3 alpha,17 beta-diol. *Proc Natl Acad Sci U S A.* **97**, 12256–12259 (2000).
17. Jacobi, G. H. *et al.* Studies on the mechanism of 3 alpha-androstanediol-induced growth of the dog prostate. *Endocrinology.* **102**, 1748–1758 (1978).
18. Khanna, M. *et al.* Substrate specificity, gene structure, and tissue-specific distribution of multiple human 3 alpha-hydroxysteroid dehydrogenases. *J Biol Chem.* **270**, 20162–20168 (1995).
19. Wilson, J. D. *et al.* 5alpha-androstane-3alpha,17beta-diol is formed in tammar wallaby pouch young testes by a pathway involving 5alpha-pregnane-3alpha,17alpha-diol-20-one as a key intermediate. *Endocrinology.* **144**, 575–580 (2003).
20. Horst, H. J. *et al.* In vivo uptake and metabolism of 3-h-5alpha-androstane-3alpha,17beta-diol and of 3-h-5alpha-androstane-3beta,17beta-diol by human prostatic hypertrophy. *Acta Endocrinol (Copenh).* **79**, 394–402 (1975).
21. Bauman, D. R. *et al.* Identification of the major oxidative 3alpha-hydroxysteroid dehydrogenase in human prostate that converts 5alpha-androstane-3alpha,17beta-diol to 5alpha-dihydrotestosterone: a potential therapeutic target for androgen-dependent disease. *Mol Endocrinol.* **20**, 444–458 (2006).
22. Chang, K. H. *et al.* Dihydrotestosterone synthesis bypasses testosterone to drive castration-resistant prostate cancer. *Proc Natl Acad Sci U S A.* **108**, 13728–13733 (2011).
23. Penning, T. M. *et al.* Pre-receptor regulation of the androgen receptor. *Mol Cell Endocrinol.* **281**, 1–8 (2008).
24. Szalay, R. *et al.* Metabolism and mode of action of androgens in target tissues of male rats. V. Uptake and metabolism of cyproterone acetate and its influence on the uptake and metabolism of testosterone and 5alpha-dihydrotestosterone in target organs and peripheral tissues. *Acta Endocrinol (Copenh).* **80**, 592–602 (1975).
25. Becker, H. *et al.* Metabolism and mode of action of androgens in target tissues of male rats. 3. Metabolism of 5 alpha-androstane-3,17-dione, of 5 alpha-androstane-3 beta,17 beta-diol and of 5 alpha-androstane-3 beta,17 beta-diol in target organs and peripheral tissues. *Acta Endocrinol (Copenh).* **73**, 407–416 (1973).
26. Krieg, M. *et al.* Binding and metabolism of 5alpha-androstane-3alpha, 17 beta-diol and of 5alpha-androstane-3beta, 17 beta-diol in the prostate, seminal vesicles and plasma of male rats: studies in vivo and in vitro. *J Endocrinol.* **64**, 529–538 (1975).
27. Morfin, R. F. *et al.* Precursors for 6beta- and 7alpha-hydroxylations of 5alpha-androstane-3beta, 17beta-diol by human normal and hyperplastic prostates. *Biochimie.* **59**, 637–644 (1977).
28. Gemzik, B. *et al.* Species differences in 5 alpha-androstane-3 beta,17 beta-diol hydroxylation by rat, monkey, and human prostate microsomes. *Arch Biochem Biophys.* **296**, 374–383 (1992).
29. Weihua, Z. *et al.* An endocrine pathway in the prostate, ERbeta, AR, 5alpha-androstane-3beta,17beta-diol, and CYP7B1, regulates prostate growth. *Proc Natl Acad Sci U S A.* **99**, 13589–13594 (2002).
30. McPherson, S. J. *et al.* Estrogen receptor-beta activated apoptosis in benign hyperplasia and cancer of the prostate is androgen independent and TNFalpha mediated. *Proc Natl Acad Sci U S A.* **107**, 3123–3128 (2010).
31. Barbier, O. & Bélanger, A. Inactivation of androgens by UDP-glucuronosyltransferases in the human prostate. *Best Pract Res Clin Endocrinol Metab.* **22**, 259–270 (2008).
32. Thompson, I. M. *et al.* The influence of finasteride on the development of prostate cancer. *N Engl J Med.* **349**, 215–224 (2003).
33. Andriole, G. L. *et al.* Effect of dutasteride on the risk of prostate cancer. *N Engl J Med.* **362**, 1192–1202 (2010).
34. Eisenberger, M. A. *et al.* Phase I and clinical pharmacology of a type I and II, 5-alpha-reductase inhibitor (LY320236) in prostate cancer: elevation of estradiol as possible mechanism of action. *Urology.* **63**, 114–119 (2004).
35. Shah, S. K. *et al.* Phase II study of dutasteride for recurrent prostate cancer during androgen deprivation therapy. *J Urol.* **181**, 621–626 (2009).
36. Huggins, C. & Hodges, C. V. Studies on prostate cancer. Effect of castration, estrogen and androgen injection on serum phosphatases in metastatic carcinoma of the prostate. *Cancer Res.* **1**, 293–297 (1941).
37. DeVore, N. M. & Scott, E. E. Structures of cytochrome P450 17A1 with prostate cancer drugs abiraterone and TOK-001. *Nature.* **482**, 116–119 (2012).
38. Veldscholte, J. *et al.* A mutation in the ligand binding domain of the androgen receptor of human LNCaP cells affects steroid binding characteristics and response to anti-androgens. *Biochem Biophys Res Commun.* **173**, 534–40 (1990).
39. Korenchuk, S. *et al.* VCaP, a cell-based model system of human prostate cancer. *In Vivo.* **15**, 163–168 (2001).
40. Takizawa, I. *et al.* Trilostane, an inhibitor of 3β-hydroxysteroid dehydrogenase, has an agonistic activity on androgen receptor in human prostate cancer cells. *Cancer Lett.* **297**, 226–230 (2010).
41. Mohler, J. L. *et al.* Activation of the androgen receptor by intratumoral bioconversion of androstanediol to dihydrotestosterone in prostate cancer. *Cancer Res.* **71**, 1486–96 (2011).
42. Muthusamy, S. *et al.* Estrogen receptor β and 17β-hydroxysteroid dehydrogenase type 6, a growth regulatory pathway that is lost in prostate cancer. *Proc Natl Acad Sci U S A.* **108**, 20090–20094 (2011).
43. Wako, K. *et al.* Expression of androgen receptor through androgen-converting enzymes is associated with biological aggressiveness in prostate cancer. *J Clin Pathol.* **61**, 448–454 (2008).

Acknowledgments

This work was supported by a Grant-in-Aid-for Scientific Research from the Ministry of Education, Culture, Sports, Science and Technology, Japan (#21592035 and #21791493), the Suzuki Foundation for Urological Medicine, and unrestricted grant from Asahi Kasei Pharma Co. We would like to thank Kenji Ohyauchi for his technical assistance.

Author contributions

F.I. and T.N. led the project and designed the experiments. F.I. and T.N. performed cell culture studies. F.I. and I.T. performed immunohistochemistry. Y.M. performed LC/MS studies. T.K. analyzed histopathology diagnoses and scored immunohistochemistry data. F.I., N.H. and T.N. interpreted the data. F.I., N.H. and T.N. drafted the manuscript. M.N. supervised throughout immunohistochemistry and histopathology diagnoses. K.T. supervised throughout the whole study.

Additional information

Competing financial interests: The authors declare no competing financial interests.

How to cite this article: Ishizaki, F. *et al.* Androgen deprivation promotes intratumoral synthesis of dihydrotestosterone from androgen metabolites in prostate cancer. *Sci. Rep.* **3**, 1528; DOI:10.1038/srep01528 (2013).